

# High-speed optical sampling using a silicon-chip temporal magnifier

Reza Salem<sup>1</sup>, Mark A. Foster<sup>1</sup>, Amy C. Turner-Foster<sup>2</sup>, David F. Geraghty<sup>1</sup>, Michal Lipson<sup>2</sup>, & Alexander L. Gaeta<sup>1</sup>

<sup>1</sup>*School of Applied and Engineering Physics, Cornell University, Ithaca, NY 14853, USA*

<sup>2</sup>*School of Electrical and Computer Engineering, Cornell University, Ithaca, NY 14853, USA*

*Corresponding author: [reza.salem@cornell.edu](mailto:reza.salem@cornell.edu)*

**Abstract:** We demonstrate a single-shot technique for optical sampling based on temporal magnification using a silicon-chip time lens. We demonstrate the largest reported temporal magnification factor yet achieved (>500) and apply this technique to perform 1.3 TS/s single-shot sampling of ultrafast waveforms and to 80-Gb/s performance monitoring. This scheme offers the potential of developing a device that can transform GHz oscilloscopes into instruments capable of measuring signals with THz bandwidths.

©2009 Optical Society of America

**OCIS codes:** (320.7100) Ultrafast measurements; (250.4745) Optical processing devices; (190.4180) Nonlinear optics, devices; (190.5970) Semiconductor nonlinear optics; (190.7110) Waveguides (230.7370).

---

## References and links

1. M. van Kampen, C. Jozsa, J. T. Kohlhepp, P. LeClair, L. Lagae, W. J. M. deJonge, and B. Koopmans, "All-optical probe of coherent spin waves," *Phys. Rev. Lett.* **88**, 227201-1-4 (2002).
2. R. W. Schoenlein, W. Z. Lin, and J. G. Fujimoto, "Femtosecond studies of nonequilibrium electronic processes in metals," *Phys. Rev. Lett.* **58**, 1680-1683 (1987).
3. M. Tonouchi, "Cutting-edge terahertz technology," *Nature Photonics* **1**, 97-105 (2007).
4. C. Dorrer, "High-speed measurements for optical telecommunication systems," *IEEE J. Sel. Top. Quantum Electron.* **12**, 843-858 (2006).
5. N. Yamada, H. Ohta, and S. Nogiwa, "Polarization-insensitive optical sampling system using two KTP crystals," *IEEE Photon. Technol. Lett.* **16**, 215-217 (2004).
6. M. Westlund, P. A. Andrekson, H. Sunnerud, J. Hansryd, and J. Li, "High-performance optical-fiber-nonlinearity-based optical waveform monitoring," *J. Lightwave Technol.* **20**, 2012-2022 (2005).
7. J. Li, M. Westlund, H. Sunnerud, B.-E. Olsson, M. Karlsson, and P. A. Andrekson, "0.5-Tb/s eye-diagram measurement by optical sampling using XPM-induced wavelength shifting in highly nonlinear fiber," *IEEE Photon. Technol. Lett.* **16**, 566-568 (2004).
8. C. Dorrer, C. R. Doerr, I. Kang, R. Ryf, J. Leuthold, and P. J. Winzer, "Measurement of eye diagrams and constellation diagrams of optical sources using linear optics and waveguide technology," *J. Lightwave Technol.* **23**, 178-186 (2005).
9. J.-H. Chung and A. M. Weiner, "Real-time detection of femtosecond optical pulse sequences via time-to-space conversion in the lightwave communications band," *J. Lightwave Technol.* **21**, 3323-3333 (2003).
10. Y. Takagi, Y. Yamada, K. Ishikawa, S. Shimizu, and S. Sakabe, "Ultrafast single-shot optical oscilloscope based on time-to-space conversion due to temporal and spatial walk-off effects in nonlinear mixing crystal," *Jpn. J. Appl. Phys.* **44**, 6546-6549 (2005).
11. P. C. Sun, Y. T. Mazurenko, and Y. Fainman, "Femtosecond pulse imaging: ultrafast optical oscilloscope," *J. Opt. Soc. Am. A* **14**, 1159-1170 (1997).
12. M. A. Foster, R. Salem, D. F. Geraghty, A. C. Turner-Foster, M. Lipson, and A. L. Gaeta, "Silicon-chip-based ultrafast optical oscilloscope," *Nature* **456**, 81-84 (2008).
13. C. Dorrer, J. Bromage, and J. D. Zuegel, "High-dynamic-range single-shot cross-correlator based on an optical pulse replicator," *Opt. Express* **16**, 13534-13544 (2008).
14. K.-L. Deng, R. J. Runser, I. Glesk, and P. R. Prucnal, "Single-shot optical sampling oscilloscope for ultrafast optical waveforms," *IEEE Photon. Technol. Lett.*, **10**, 397-399 (1998).
15. J. Chou, O. Boyraz, B. Jalali, "Femtosecond real-time single-shot digitizer," *Appl. Phys. Lett.* **91**, 161105 (2007).
16. C. Dorrer, "Single-shot measurement of the electric field of optical waveforms by use of time magnification and heterodyning," *Opt. Lett.* **31**, 540-542 (2006).

17. S. A. Akhmanov, V. A. Vysloukh, and A. S. Chirkin, "Self-action of wave packets in a nonlinear medium and femtosecond laser pulse generation," *Sov. Phys. Usp.* **29**, 642-677 (1986).
18. B. H. Kolner, "Space-time duality and the theory of temporal imaging," *IEEE J. Quantum Electron.* **30**, 1951-1963 (1994).
19. M. T. Kauffman, W. C. Banyal, A. A. Godil, and D. M. Bloom, D. M. "Time-to-frequency converter for measuring picosecond optical pulses," *Appl. Phys. Lett.* **64**, 270-272 (1994).
20. J. van Howe and C. Xu, "Ultrafast optical signal processing based upon space-time dualities," *J. Lightwave Technol.* **24**, 2649-2662 (2006).
21. C. V. Bennett and B. H. Kolner, "Principles of parametric temporal imaging - Part I: System configurations," *IEEE J. Quantum Electron.* **36**, 430-437 (2000).
22. C. V. Bennett, R. P. Scott, and B. H. Kolner, "Temporal magnification and reversal of 100 Gb/s optical data with an upconversion time microscope," *Appl. Phys. Lett.* **65**, 2513-2515 (1994).
23. C. V. Bennett, B. D. Moran, C. Langrock, M. M. Fejer, and M. Ibsen, "640 GHz real-time recording using temporal imaging," *Conference on Lasers and Electro-Optics, OSA Technical Digest CD*, paper CtuA6 (2008).
24. R. Salem, M. A. Foster, A. C. Turner, D. F. Geraghty, M. Lipson, and A. L. Gaeta, "Optical time lens based on four-wave mixing on a silicon chip," *Opt. Lett.* **33**, 1047-1049 (2008).
25. R. L. Espinola, J. I. Dadap, R. M. Osgood, Jr., S. J. McNab, and Y. A. Vlasov, "C-band wavelength conversion in silicon photonic wire waveguides," *Opt. Express* **13**, 4341-4349 (2005).
26. Y.-H. Kuo, H. Rong, V. Sih, S. Xu, and M. Paniccia, "Demonstration of wavelength conversion at 40 Gb/s data rate in silicon waveguides," *Opt. Express* **14**, 11721-11726 (2006).
27. M. A. Foster, A. C. Turner, J. E. Sharping, B. S. Schmidt, M. Lipson, and A. L. Gaeta, "Broad-band optical parametric gain on a silicon photonic chip," *Nature* **441**, 960-963 (2006).
28. M. A. Foster, A. C. Turner, R. Salem, M. Lipson, and A. L. Gaeta, "Broad-band continuous-wave parametric wavelength conversion in silicon nanowaveguides," *Opt. Express* **15**, 12949-12958 (2007).
29. A. C. Turner, M. A. Foster, B. S. Schmidt, A. L. Gaeta, and M. Lipson, "Tailored anomalous group-velocity dispersion in silicon channel waveguides," *Opt. Express* **14**, 4357-4362 (2006).
30. J. Azana and M. A. Muriel, "Real-time optical spectrum analysis based on the time-space duality in chirped fiber gratings," *IEEE J. Quantum Electron.* **36**, 517-526 (2000).
31. Y. Han and B. Jalali, "Time-bandwidth product of the photonic time stretch analog-to-digital converter," *IEEE Trans. Microwave Theory Tech.* **51**, 1886-1892 (2003).

## 1. Introduction

Characterizing ultrafast optical signals has far-reaching applications in many areas of science and technology such as ultrafast phenomena [1,2], terahertz spectroscopy [3], and ultrahigh-bandwidth communications [4-8]. The traditional optoelectronic approach for optical signal sampling uses high-speed detectors and sample-and-hold circuits, which cannot be applied to signals that have excessively large bandwidths. One approach proposed to overcome this bandwidth problem is based on performing a cross-correlation with a short optical pulse train [4-8]. Various techniques for cross-correlation have been demonstrated and are based primarily on a form of nonlinear optical gating [5-7]. For example, nonlinear processes such as sum- and difference-frequency generation [5], four-wave mixing (FWM) [6], and cross-phase modulation [7] have been used for sampling communication signals at data rates as high as 500 Gb/s. Cross-correlation based on coherent linear detection has also been studied [8] and is architecturally similar to these nonlinear techniques. While such systems can achieve sub-picosecond sampling resolution, the sample points are far apart in time since they are determined by the sampling pulse period (longer than a nanosecond). As a result, the samples must be post-processed in order to reconstruct a repetitive waveform or the eye diagram corresponding to a digital data stream. Optical packets and non-repetitive optical waveforms cannot be characterized using these sampling techniques, and rapid fluctuations in the signal are difficult to monitor and characterize because each pump pulse arrival generates only a single point in the sampled waveform. Several solutions have been proposed that are capable of characterizing arbitrary waveforms in a single shot. One solution is time-to-space conversion, which allows temporal sampling using an array of detectors [9-12]. However, most of the demonstrated systems based on this approach have limited waveform record length, and it is difficult to achieve fast detector read-out rates, which makes them unsuitable for monitoring rapidly varying signals. Another solution is based on creating several replicas of the pump signal [13] or the input waveform [14] in order to perform single-shot sampling.

However, the sensitivity is limited by the number of the created replicas, which leads to a trade-off between sensitivity and the number of samples.

## 2. Operation principle

A fundamentally different approach for high-speed sampling is to stretch the input signal in time, similar to the technique used for optical sampling of electrical signals [15,16]. In this work, we report results demonstrating optical sampling based on temporal stretching using a FWM time lens. Our scheme uses the concept of space-time duality [12,17-23], which relies upon the equivalence between the diffractive propagation of a spatial field and the dispersive propagation of a temporal waveform. Much like a spatial lens can magnify a spatial pattern, a temporal lens can magnify a signal in time [21-24]. The function of the lens in the time domain is to impart a quadratic phase shift on the input signal, and the most straightforward approach would be to use an electro-optic phase modulator. However the maximum phase shift that can be imparted on the signal is limited, which restricts its use for ultrafast signal processing [19-21]. An alternative approach for creating a time lens that can produce more than 10 times the maximum phase shift as compared to an electrically-driven phase modulator is based on utilizing a parametric nonlinear optical process such as sum- or difference-frequency generation with a chirped pump pulse [21-23]. The quadratic phase of the chirped pump pulse is transferred to the input signal through the nonlinear wave mixing process, and temporal imaging schemes have been demonstrated using this approach [21-23]. In recent work, we demonstrated that FWM in a silicon waveguide can also be used to realize a parametric time lens [12,24]. Unlike the sum- and difference-frequency generation, the input and output signals are in the telecommunications band. Here, we demonstrate the utility of a FWM-based time lens for temporal stretching of high-speed signals by factors as large as 520, such that the sampling can be performed using low-speed electronic devices. We also show single-shot sampling at sampling rates exceeding 1 TS/s and performance monitoring at 80 Gb/s as two important applications of this device. The read-out rates achieved using this scheme approach nanosecond time scales, which allows for characterization of rapidly-varying signals. The implementation that we report is a fully-guided system that utilizes a silicon nanowaveguide, based on the CMOS-compatible silicon-on-insulator technology, and commercially-available single-mode optical fibers. In addition to their robust and electronics-compatible platform with a standard fabrication process, silicon waveguide devices allow power-efficient [25-28] and broadband [27,28] wavelength conversion via dispersion engineering [29], such that temporal resolutions less than 100 fs are possible.

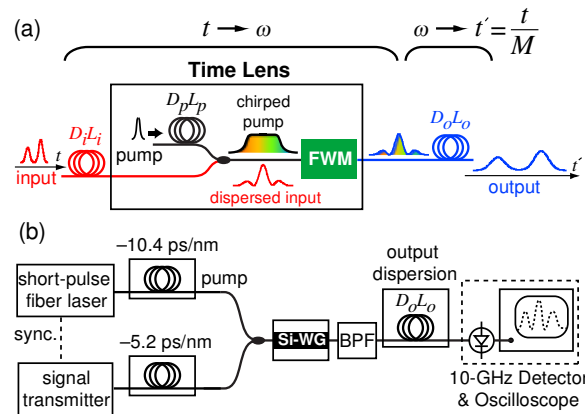


Fig. 1. (a) Schematic diagram showing the concept of temporal magnification using the FWM time lens. A chirped pump pulse is mixed with the input signal, which transfers a quadratic phase to the signal. (b) Experimental setup used to demonstrate the temporal magnification concept using a silicon nanowaveguide.

Figure 1(a) shows a schematic of the temporal stretching system consisting of an input dispersive element, a time lens, and an output dispersive element. The time lens is comprised of a pump pulse that is chirped by passing through a dispersive element and a silicon nanowaveguide that transfers the linear chirp of the pump pulse to the dispersed input signal via FWM. In a manner similar to the way that a spatial imaging system magnifies spatial patterns, the input signal is magnified in time and the magnification factor is given by  $M = D_o L_o / D_i L_i$ , where  $D_i L_i$  and  $D_o L_o$  are the total dispersion of the input and output dispersive elements, respectively. For large stretching factors the total input dispersion ( $D_i L_i$ ) should be approximately half of the dispersion used for chirping the pump pulse ( $D_p L_p$ ), which corresponds to the temporal focal length of the time lens [12,24]. Similar to a spatial Fourier analyzer, the spectrum of the signal after the time lens represents the temporal input waveform with the time-to-wavelength conversion factor given by  $\Delta\lambda/\Delta t = (D_i L_i)^{-1}$ . Analogous to Fraunhofer diffraction, the large dispersive element after the time lens converts the signal from the frequency domain back to the time domain [30] with wavelength-to-time conversion factor approximately given by  $\Delta t'/\Delta\lambda = D_o L_o$ , which results in the temporal stretching factor  $M = D_o L_o / D_i L_i$  between  $t$  and  $t'$ .

### 3. Experiment

The experimental setup used for demonstrating this technique is shown in Fig. 1(b). A passively mode-locked fiber laser with 38-MHz repetition rate and 7-nm bandwidth is used as the pump source and is followed by a length of dispersion-compensating fiber with total dispersion  $D_p L_p = -10.4$  ps/nm. The input signal is sent through another length of dispersion-compensating fiber with total dispersion  $D_i L_i = -5.2$  ps/nm and is combined with the chirped pump pulse. The combined pump and signal are sent into the silicon nanowire (300 nm  $\times$  700 nm cross-sectional dimensions and 1.8-cm long), and the idler component generated by the FWM process is separated using a bandpass filter and sent into a dispersion-compensating module with a total dispersion equal to  $D_o L_o$ . The stretched signal is then detected with a 10-GHz detector and measured using a 10-GHz sampling oscilloscope. The silicon nanowaveguide is fabricated on an SOI platform using E-beam lithography, and the average linear propagation loss is 2 dB/cm. The light is coupled into the waveguide using a lensed single-mode fiber, and the waveguide output is coupled back into an optical fiber using a microscope objective lens. The coupling loss on each waveguide facet is approximately 4 dB. The dispersion compensating fiber used in the system (Corning model: DCM-D-080-04) has a dispersion parameter of  $D = 87$  ps/nm<sup>2</sup>·km and a dispersion slope of  $S = 0.025$  ps/nm<sup>2</sup>·km. The ratio of the dispersion slope ( $S$ ) to the dispersion parameter ( $D$ ) for this fiber is 12 times smaller than that of the standard single-mode fiber, which minimizes the distortions caused by the third-order dispersion.

In the first experiment, we use a repetitive signal that consists of two 3-ps pulses separated by 8.7 ps in order to demonstrate the concept of temporal stretching. The signal and pump are generated from the same fiber laser by spectral filtering. Figure 2(a) shows the cross-correlation of the input signal with an ultrafast pump, and Fig. 2(b) shows the spectrum at the output of the silicon waveguide. As seen in Fig. 2(b), the idler spectrum represents the signal in the time domain, which demonstrates the time-to-frequency conversion after the time lens. The stretched signal measured on a 10-GHz sampling oscilloscope is plotted in Fig. 2(c) for three different values of the output dispersion ( $D_o L_o$ ) demonstrating both positive and negative stretching factors. We also utilize this scheme for characterizing more complex waveforms such as the one shown in Fig. 2(d). The complex waveform is generated by partially overlapping two pulses (4-nm spectral width and centered at 1536 nm) in time and sending them into a 300-m spool of standard single-mode fiber. The waveform is stretched by a factor of 520 (to our knowledge, the largest time stretching factor demonstrated experimentally) using  $D_o L_o = -2720$  ps/nm and is compared with its cross-correlation. Our numerical modelling of the system for  $M = 520$  shows a 330-fs impulse response, which is in agreement with the simplified model [12] that assumes zero dispersion slope and a very large magnification factor in order to reach the Fraunhofer limit. Based on this estimated resolution

and the time aperture of the measurement determined by the width of the chirped pump pulse ( $\sim 70$  ps), we estimate the record-length-to-resolution ratio (or the time-bandwidth product [31]) of the measurement to be 210.

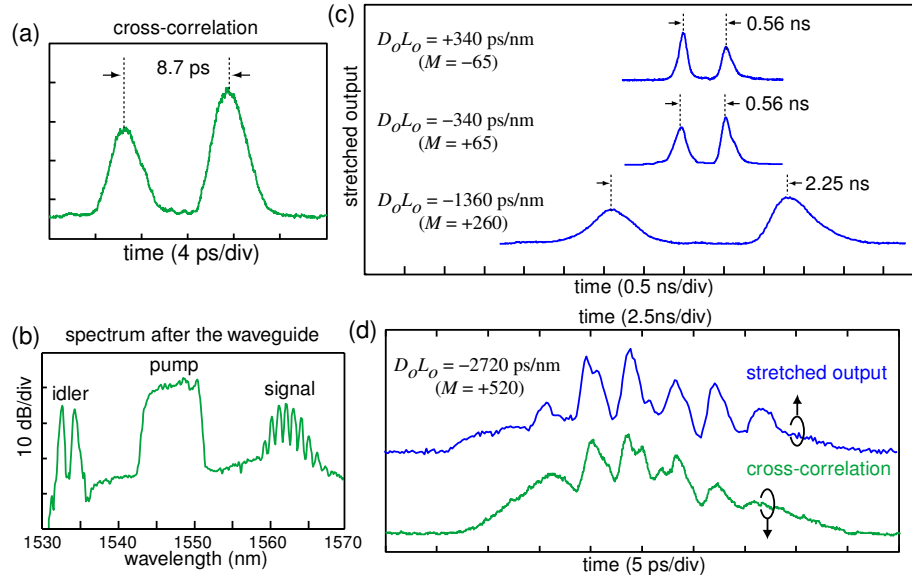


Fig. 2. (a) Cross-correlation of the first signal under test. (b) Optical spectrum measured at the output of the silicon waveguide showing an efficient wavelength conversion. The converted signal spectrum represents the input waveform in the time domain (time-to-frequency conversion). (c) Stretched signal shown for different magnification factors. (d) An arbitrary optical waveform shown before and after the temporal stretching by a factor of 520.

We can also use this system for single-shot measurements of randomly varying waveforms. Figure 3(a) shows how this scheme can be used for sampling a randomly encoded data stream. The measurement window is determined by the width of the chirped pump pulse ( $\sim 70$  ps in this case), which can be adjusted by choosing the amount of dispersion on the pump path. The signal inside of this measurement window is stretched and measured using a detector and a real-time oscilloscope. We generate a 10-GHz pulse train using a standard Mach-Zehnder pulse carver, which produces 33-ps pulses, and a time-lens compressor that compresses the pulses down to 4.5 ps. The pulse train is then modulated using a 10-Gb/s pattern generator with  $2^{31}-1$  pattern length. The signal is time-interleaved with its delayed copy such that the delay between the adjacent bits is 12.5 ps simulating an 80-Gb/s RZ data stream. The signal source is synchronized to the fiber laser, which is used as the pump source. Figure 3(b) shows a plot of the stretched signal sampled on a 5-GHz real-time oscilloscope at 20 GS/s, which demonstrates the single-shot capability of the scheme. The signal is stretched by a factor of  $M = 65$  ( $D_oL_o = -340$  ps/nm), which corresponds to a 1.3-TS/s sampling rate or a 770-fs spacing between the samples. The eye diagram is generated using 380 snap-shots of the input signal (approximately 8000 samples) accumulated over a 10- $\mu$ s time window and is plotted in Fig. 3(b), showing a clear open eye for the 80-Gb/s data rate. By increasing the dispersion after the time lens to  $D_oL_o = -1360$  ps/nm ( $M = 260$ ), we demonstrate a 5.2 TS/s sampling rate using the 5-GHz (20-GS/s) oscilloscope and a 1.3-TS/s sampling rate using a slower 1-GHz (5-GS/s) oscilloscope. One of the main applications of the high-speed sampling systems is to monitor the performance of communication channels and transmitters. Here, we show the utility of this scheme for monitoring the performance of our transmitter. We use three different pulse widths (4.5 ps, 6 ps, and 7 ps) in order to see the effect of the interference between the adjacent bits. The longer pulses are generated by adjusting the time-lens compressor to produce weaker compression. The eye diagrams corresponding to these three pulse widths are plotted in Fig. 4, which shows signal degradation for longer pulses. The

power sensitivity of the measurement is determined by the minimum detectable output peak power, which depends on the magnification factor. For the measurements shown in Fig. 3 in which  $M = 62$ , the estimated minimum input peak power is 5 mW. This value can be lowered by increasing the FWM conversion efficiency and the waveguide coupling efficiency.

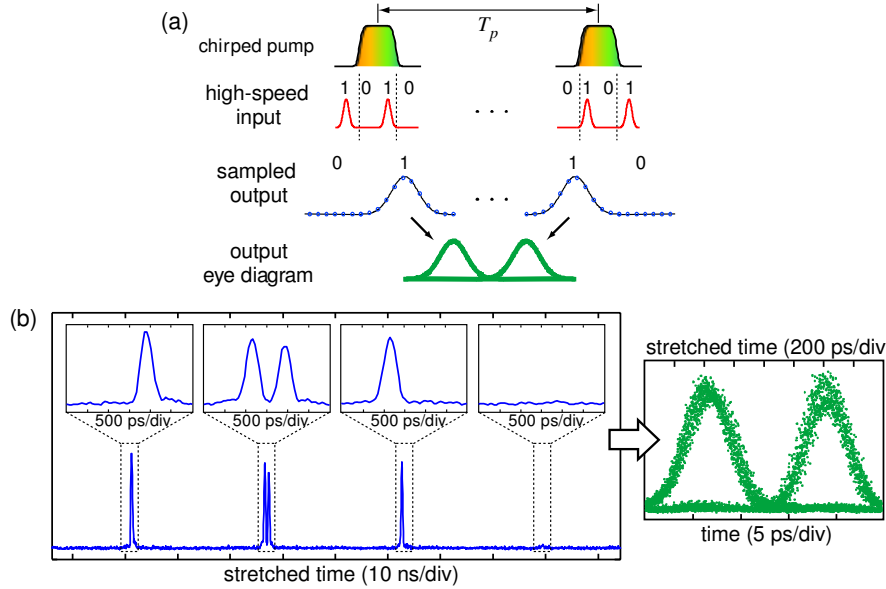


Fig. 3. (a) Schematic showing the application of the time stretching scheme for characterizing randomly varying signals. (b) Single-shot measurement of an 80-Gb/s RZ signal and the corresponding eye diagram.

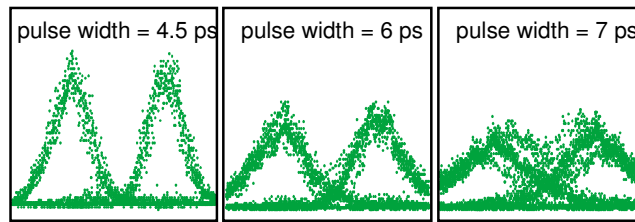


Fig. 4. Eye diagram comparison for three different pulse width settings of the transmitter showing a degraded eye diagram for longer pulse widths

#### 4. Summary

In summary, we have demonstrated a high-speed sampling scheme based on temporal magnification of the signal by factors larger than 500. Our approach allows optical sampling at rates larger than 1-TS/s using a 1-GHz oscilloscope. Unlike conventional optical sampling techniques, this method allows single-shot sampling and the measurement of short optical packets. In addition, eye diagrams can be generated within a  $\mu\text{s}$  time-scale, which allows monitoring MHz-rate variations in the input signal.

#### Acknowledgments

We acknowledge financial support from the DARPA DSO OAWG Program and the Center for Nanoscale Systems, supported by the NSF and the New York State Office of Science, Technology & Academic Research. This work was performed in part at the Cornell NanoScale Facility, a member of the National Nanotechnology Infrastructure Network, which is supported by the National Science Foundation (Grant ECS-0335765).